Surface Flashover over a Micro-Profiled Cylinder in Air

Hans Kristian Meyer, Robert Marskar, Helene Osberg, Frank Mauseth*

Abstract

Increasing the lightning impulse (LI) flashover voltage of insulators can require significant changes to the geometry and material properties of the insulator or electrodes. In some cases, such changes can be difficult to implement as they may require more volume or may compromise e.g. mechanical properties of the insulating parts. In this work, a new micro-scale surface profile which inhibits streamer discharge propagation without introducing major changes to the insulation system geometry or materials is demonstrated. Polyoxymethylene (POM) cylinders with 25 % glass fibre in air were machined with 0.5x0.4 mm rectangular grooves spaced 0.6 mm apart and stressed with LIs. A non-profiled cylinder and a cylinder with a larger, semi-circular grooves were tested for comparison. The cylinders were tested in a 48.5 mm atmospheric air gap with an exposed triple junction as the positive electrode. The rectangular surface profiles increased the LI flashover voltage ($U_{50\%}$) from 70.0 to 96.5 kV_{peak}. High-speed imaging showed positive surface streamer discharges stopping on the surface profiles. Discharge inception calculations were used to explain the influence of the surface profile on the flashover process. The results are relevant for technological applications with electrically stressed solid insulators in gases.

1 Introduction

Replacing SF_6 in gas-insulated high voltage devices with non-greenhouse gases such as air requires re-design and optimization of the electrical insulation system. Typically, the geometry or pressure is changed such that

*Hans Kristian Meyer and Robert Marskar are with SINTEF Energy Research, Trondheim, Norway. Helene Osberg and Frank Mauseth are with NTNU - Norwegian University of Science and Technology, Trondheim, Norway.

Author Accepted Manuscript version of the article by Hans Kristian Meyer et al. in
IEEE Transactions on Dielectrics and Electrical Insulation, (2023), DOI: http://dx.doi.org/10.1109/TDEI.2023.3277413

electrical discharge inception is prevented everywhere in the new gas. However, allowing discharge inception under some transient overvoltage conditions can result in more compact insulation systems. For lightning impulse (LI) withstand tests, non-disruptive discharges are acceptable, as the stress duration is short. This is not the case for power frequency (ac) tests, where discharge activity will likely be repeated over several voltage cycles and may cause deterioration of the insulation materials. For gas-insulated devices, LI tests are often more challenging than ac tests, as the peak voltage value is much higher, and as the breakdown (BD) phenomena are fast.

1.1 Breakdown mechanisms in air

For medium-voltage gas-insulated devices such as metal-enclosed switchgear, the electric field stresses are non-homogeneous, with inter-electrode distances of typically a few cm. Moreover, gas-metal, gas-dielectric, and gas-metal-dielectric interfaces (i.e. triple junctions) are typically present.

One important discharge mechanism in such insulation systems is the streamer discharge. Streamers are low-temperature plasma filaments that propagate in relatively low background electric fields once initiated. The necessary voltage for streamer initiation can be estimated with electrostatic field calculations and semi-empirical criteria [1]. Streamers that propagate in the direction of the electric field are called positive streamers or cathode-directed streamers, while streamers propagating against the field direction are called negative or anode-directed. In atmospheric air, positive streamers are more critical, i.e. they initiate at lower voltage stresses and propagate further than negative streamers.

Streamers are not necessarily disruptive, i.e. they do not necessarily lead to a voltage collapse, even when they connect the live electrode to ground. Streamers can become disruptive if they transition to a high-temperature discharge such as a spark or a leader [2, 3].

1.2 Flashover over solid dielectric surfaces in air

In air-insulated devices, electrical discharge propagation can be inhibited or aided by solid dielectric surfaces, depending on the electric field, solid dielectric geometry and material properties. Inception of surface streamers from triple junctions can be critical in some insulation systems, especially in cases where the background field direction is tangential to the dielectric surface. Surface streamers are faster than air streamers, but can also require higher background fields to sustain propagation [4]. Furthermore, accumulated charges on dielectric surfaces can play an important role in the surface

flashover process, both transiently during a discharge event, and as a memory effect from previous discharges [5, 6].

Reducing tangential electrical field stresses and shielding triple junctions can suppress surface discharges and flashover. Dielectric barriers, electrode coatings or sheds can also be used to increase the withstand voltage of gaseous insulation systems. For example, sheds on cylinders typically reduce both streamer propagation range and the surface flashover probability [4, 7]. Such sheds are especially useful in environments where the insulator can be contaminated with e.g. water or dust. Other known techniques for increasing surface flashover voltage include insulator surface coating, etching or roughening techniques [8, 9]. The process leading to surface flashover over insulating cylinders is, however, not well understood. It is typically assumed that flashover occurs when a sufficient amount of energy is deposited in the streamer channels [4], or when a so-called secondary streamer is initiated [10].

One less-explored alternative is to use small-scale profiles on dielectric surfaces to suppress streamer propagation along the surface in air. Such profiles may not be well suited for very contaminated environments, but could be effective in insulation systems with a controlled atmosphere such as gas-insulated switchgear. Small, regular grooves have been demonstrated to increase the flashover voltage over insulators in vacuum insulation systems [8, 11]. It is also generally known that profiles on smaller spatial scales may have an impact on triple-junction effects and charge accumulation [12]. Nevertheless, there is not much literature on the use of micro-profiles on insulator surfaces to increase LI flashover voltage by stopping streamer propgation in gas-insulated systems. It was shown in previous work by the authors that streamer propagation is inhibited by surface profiles that are of a similar spatial scale as the streamer front, which is a few hundred microns in atmospheric air [13, 14]. Rectangular-cut grooves with such dimensions were strongly streamer-inhibiting, in both simulations and experiments.

The main goal of this work is to therefore test whether such small-scale surface profiles on a cylindrical insulator with tangential electric field stress can increase LI flashover voltage in ambient air. Another goal is to gain insights into the physical mechanisms leading to LI flashover over non-profiled and profiled cylinders in ambient air.

2 Methods

2.1 Preparation of test objects

Electrodes were made from aluminium, and the arrangement is shown in Fig. 1. A toroidal field controller was used to shield the triple junction on the upper side of the cylinder, where the impulse voltage was applied. On the opposite electrode, a sharp, asymmetrical ring protruding 2.5 mm was placed. This ring was shifted 2.5 mm from the center axis of the cylinder, such that an unshielded triple junction was created on one side of the cylinder. This arrangement was made to get a small region where discharges start, to facilitate high-speed imaging.

Polyoxymethylene (POM) cylinders with 25 % glass fibre ($\epsilon_r = 4.3$) with 30 mm diameter were tested in the setup. This material was chosen to represent an insulating material with mechanical strength and moderate relative permittivity which could be machined with fine-detailed surface profiles. Profiles were machined on the cylinder surface, with similar dimensions as the rectangular-cut profiles in previous work [14,15]. A non-profiled cylinder and a cylinder with a semi-circular profile with larger dimensions were tested for comparison. The average roughness of the non-profiled cylinder was measured with a profilometer to around 1.5 µm. The surface profile dimensions of the profiled cylinder were also measured with a profilometer, with average values shown in Fig. 1, rounded to nearest 0.1 mm.

The cylinders were mounted manually with set screws, and as there were mechanical tolerances on the dimensions shown in Fig. 1, small air gaps (0.1-0.2 mm) could be present near triple junctions, such that the triple junctions were not always perfect gas-metal-dielectric interfaces. Furthermore, with the profiled surfaces, the location of the profiles relative to triple junctions was not controlled.

2.2 Experimental setups

LI breakdown tests were performed with 1 minute waiting time between shots. The sharp electrode edge was grounded and was the positive electrode, which represents the most critical field direction for flashover in inhomogeneous air gaps.

The cylinders were tested in two different setups, see Fig. 2. In the first setup, Fig. 2a, a 200 kV two-stage LI generator with 0.5 μF capacitors (High Volt model IPF 5 / 200 L) was used to apply standard 1.2/50 μs LIs, and voltage was measured with a North Star PVM-100 probe over the test object. In a second setup, Fig. 2b, two 1 μF capacitor stages of a 1.2 MV, High Volt

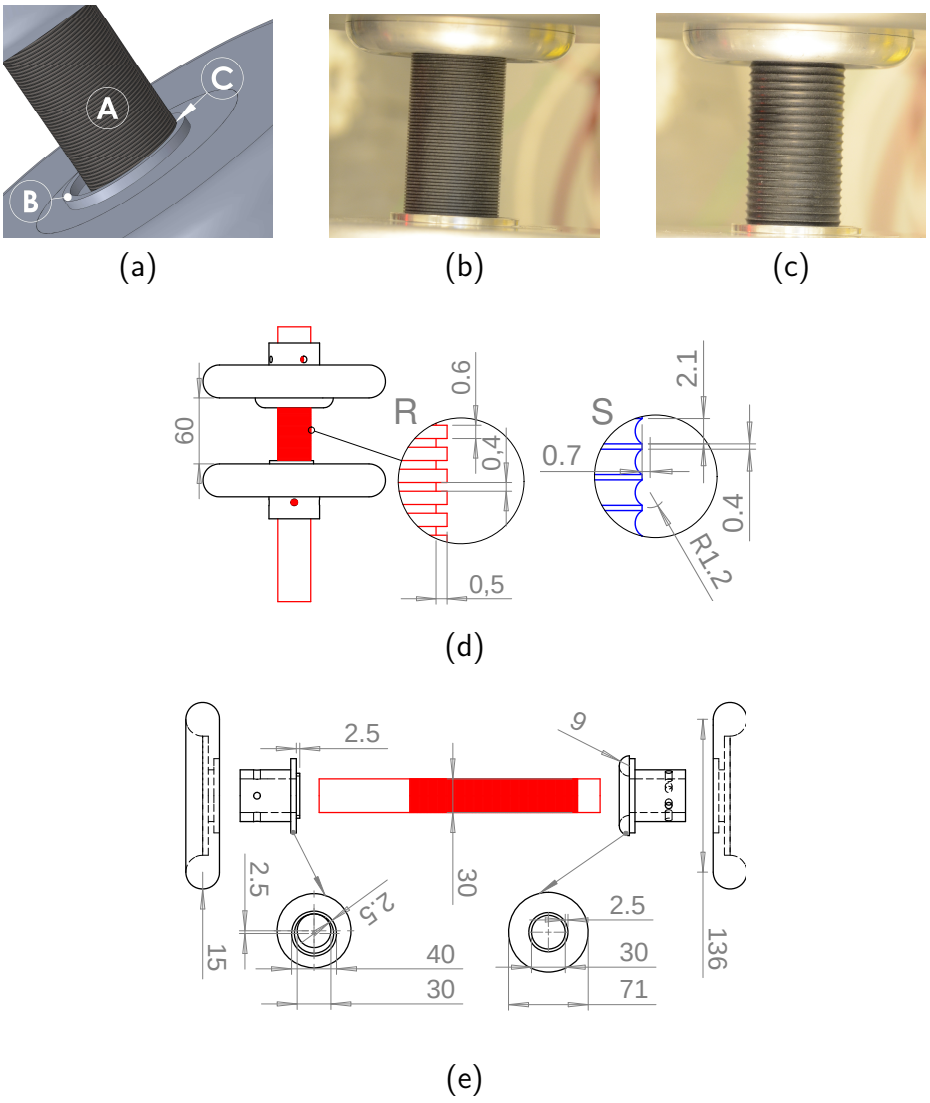

Figure 1: Test object illustration, images and drawings with dimensions (all units in mm). a) 3D model of test object with rectangular-profiled insulator (A), asymmetric electrode (B) and exposed triple junction (C). b) image of the prepared test object with rectangular profile "R". c) image of the prepared test object with semi-circular profile "S". d) Overview of test object with detail of surface profiles (showing profile "R" in red color and profile "S" in blue color), side view. e) "exploded" view of cylinder and electrodes (side view) and details of the rounded high-voltage electrode and asymmetrical grounded electrode (top view). The red- and blue-colored parts are insulators, all other parts are machined from aluminium.

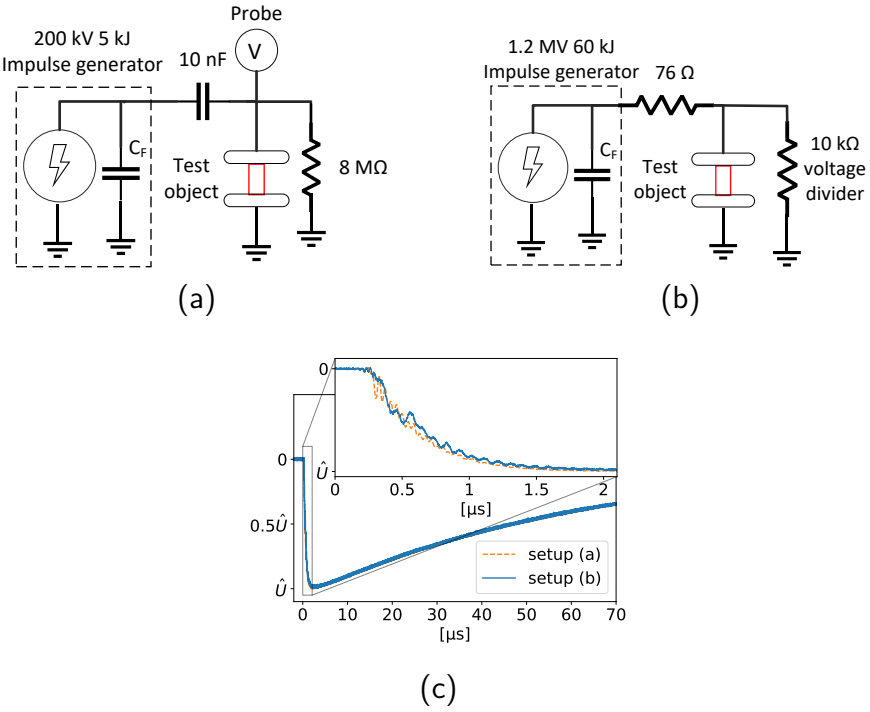

Figure 2: a) Setup used for breakdown testing, b) setup used for high-speed imaging and breakdown testing, c) voltage shapes in the two setups, scaled to peak voltage value $\hat{U}$, with inset showing the impulse front.

IP 60 / 1200 L generator were used. High-speed intensified images of the flashover process were taken in the Fig. 2b setup using the imaging setup described in [14]. The images were post-processed by adjusting brightness, contrast and color look-up table, and by overlaying an illuminated picture of the setup. A photo-multiplier tube (PMT) of type Philips 56AVP photo-multiplier tube (PMT) with a spectral range of 380 to 680 nm was used for discharge detection. The signal propagation delay in cabling and intensifier units (PMT and camera) was compensated for when post-processing signal. The voltage shapes of both setups are shown in Fig. 2c.

2.3 Test procedure

Surface charges are difficult to remove, especially on small-scale profiles. A test procedure similar to the one in [16] was used in an attempt to randomize the influence of surface charge. First, the 50 % breakdown voltage ($U_{50\%}$) was estimated with the up-and-down method [17]. Thereafter, LIs were applied in a random order with a resolution of 0.2 kV charging voltage within an

interval around the estimated $U_{50\%}$. The test voltage interval was adjusted a few times as the initial interval did not cover the whole distribution.

The data was grouped into bins of 6 kV, and the relative frequency of breakdown for each bin was found (i.e. the number of breakdowns divided by the number of trials). The relative frequencies were then used as point estimates for the breakdown probability at the mean voltage values of each bin. Two-sided 95 % confidence intervals of each point estimate were calculated.

The test objects were conditioned with several breakdowns before testing. The breakdown data was not corrected for atmospheric conditions. The relative humidity, temperature and pressure varied between 17-29 %, 20-23 °C and 973-1010 hPa respectively during the experiments.

2.4 Streamer inception calculations

The voltage required for streamer inception along an electric field line L can be estimated by integrating the field- and pressure-dependent effective ionization coefficient $\overline{\alpha}(\mathbf{E}, p)$:

$$\int_L \overline{\alpha}(\mathbf{E}, p) d\mathrm{l} > \ln(N_{\mathrm{crit}}), \tag{1}$$

where $\mathbf{E}$ is the electric field strength, p is the pressure and N_{crit} is the critical size of an electron avalanche. Equation 1 was evaluated over selected field lines from a 3D finite element method (FEM) electrostatic simulation using $\ln(N_{\mathrm{crit}}) = 9$. The integration was started from the electrode and stopped when $\overline{\alpha}(\mathbf{E}, p) = 0$. Values for $\overline{\alpha}(\mathbf{E}, p)$ from [18] were used.

The COMSOL 3D simulation domain and boundary conditions are shown in Fig. 3. In the simulation model, surface profiles were only added near the sharp electrode to reduce the mesh amount. The edges of the dielectric surface profiles, as well as the sharp electrode edges and triple junctions were rounded with 0.1 mm. It was difficult to obtain good profilometer measurements of the sharp edge of the grounded electrode in Fig. 1, but 0.1 mm rounding of the edge was an acceptable approximation to the measurements. For more details on the effect of sharp edges on streamer inception calculations and experiments, see [16].

3 Results and Discussion

3.1 Surface profile effect on flashover probability

The breakdown data for the non-profiled, R-profiled and S-profiled cylinders are shown in tables 1, 2 and 3 respectively. The voltage range and mean

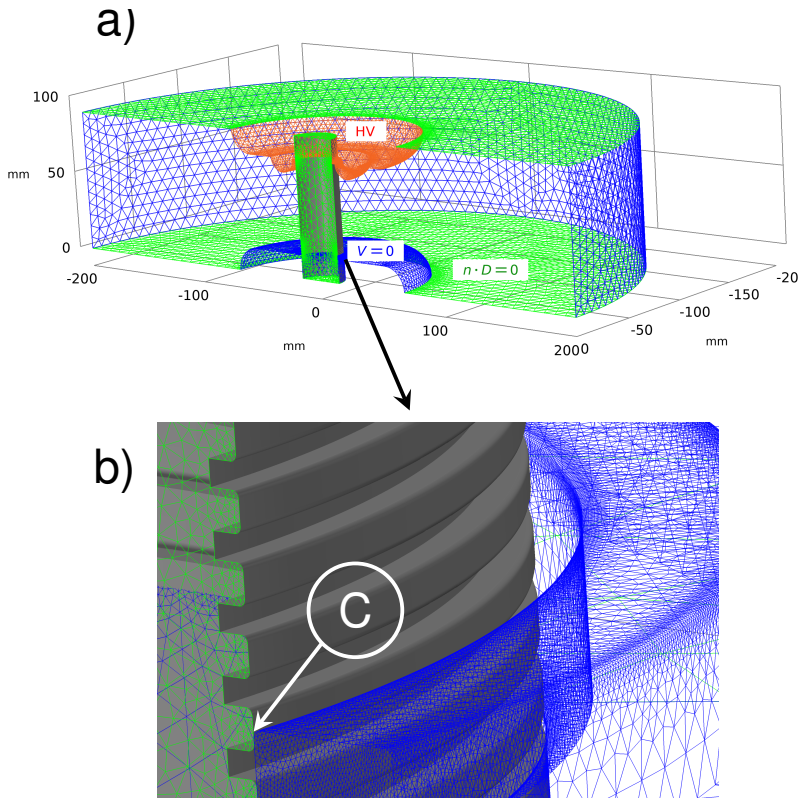

Figure 3: Simulation boundary conditions and surface mesh with color coding (red: high voltage $V = \hat{U}$, blue: ground $V = 0$, green: zero charge boundary $n \cdot D = 0$). a) Entire simulation domain. The open wall also has a zero charge condition, to make use of the symmetry in the test object and reduce the mesh amount. The grounded half-cylinder surface around the setup imitates the effect of the grounded wall in the laboratory. b) Magnified region around triple junction (C), also showing the small-scale rectangular profiles.

voltage of each bin is shown in the first column, the number of non-BDs and BDs of each bin in the second and third column respectively, and the relative breakdown frequency of each bin with upper and lower 95 % confidence intervals (CIs) in the fourth column. The same data is plotted in Fig. 4, where it can be seen that the breakdown voltage is significantly increased for the R-profiled surface. $U_{50\%}$, for example, increases from 70 kV to 96.5 kV. Normal distribution curves were fitted to the data as shown in Fig. 4. The S-profile does not increase the breakdown voltage significantly, because this type of profile does not inhibit streamer propagation as the R-profile does.

Table 1: Non-profiled cylinder breakdown data

Range (mean) [kV]	non-BDs	BDs	Rel. freq. (95% CI)
50-56 (53.7)	11	0	(0.00) 0.00 (0.28)
56-62 (59.7)	44	0	(0.00) 0.00 (0.08)
62-68 (65.4)	54	12	(0.10) 0.18 (0.30)
68-74 (70.3)	24	22	(0.33) 0.48 (0.63)
74-80 (77.7)	5	40	(0.76) 0.89 (0.96)
80-86 (83.2)	0	10	(0.69) 1.00 (1.00)
86-92 (88.8)	0	16	(0.79) 1.00 (1.00)
92-98 (93.8)	0	9	(0.66) 1.00 (1.00)

Table 2: Rectangular micro-profiled (Profile R) cylinder breakdown data

Range (mean) [kV]	non-BDs	BDs	Rel. freq. (95% CI)
70-76 (71.9)	4	0	(0.00) 0.00 (0.60)
76-82 (79.4)	43	1	(0.00) 0.02 (0.12)
82-88 (84.9)	64	5	(0.02) 0.07 (0.16)
88-94 (90.4)	30	9	(0.11) 0.23 (0.39)
94-100 (96.1)	18	14	(0.26) 0.44 (0.62)
100-106 (102.1)	2	19	(0.70) 0.90 (0.99)
106-112 (108.8)	0	9	(0.66) 1.00 (1.00)

Table 3: Semi-cirular profiled (Profile S) cylinder breakdown data

Range (mean) [kV]	non-BDs	BDs	Rel. freq. (95% CI)
54-60 (58.9)	4	0	(0.00) 0.00 (0.60)
60-66 (63.1)	25	0	(0.00) 0.00 (0.14)
66-72 (68.9)	21	6	(0.09) 0.22 (0.42)
72-78 (74.6)	2	32	(0.80) 0.94 (0.99)
78-84 (79.7)	0	10	(0.69) 1.00 (1.00)

3.2 High-speed images

The high-speed images in Fig. 5 show surface streamers stopping on the profiled cylinder, with no flashover occuring. In Fig. 5a, the streamers stop in one of the first grooves. A similar discharge is also seen in Fig. 5b, but here one of the streamers propagates over several grooves before stopping. Note that the streamers typically propagate laterally along the grooves. The

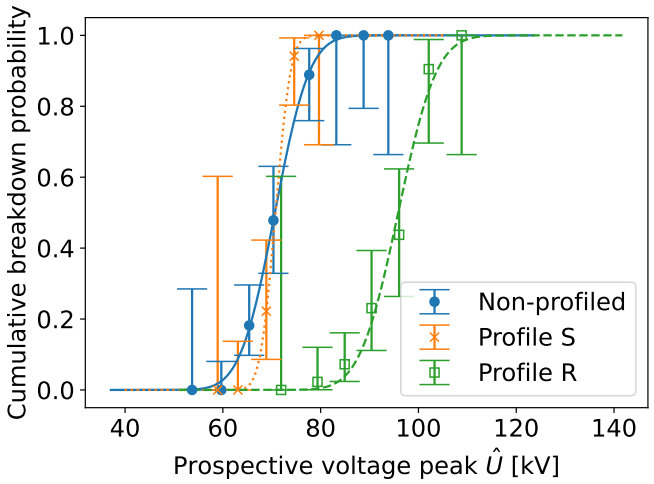

Figure 4: The breakdown voltage increases when the cylinder surface is profiled with small-scale rectangular-cut grooves (Profile R), but not when cut with larger, semi-circular grooves (Profile S). Cumulative breakdown probability with data points (sorted into 6 kV bins) and 95 % confidence intervals for the point estimates (data in tables 1 and 2). The curves are normal distribution fits to the data.

oscilloscope traces in Fig. 6a show that the discharge in Fig 5b happened on the falling voltage flank, that the camera gating time captured all discharge activity during the impulse, and that there was no voltage collapse.

In previous work by the authors [14], fluid simulations and high-speed imaging were used to provide a theoretical explanation on the mechanisms of streamer-stopping on such profiles, although in a different field configuration. In that work the R-profile was also compared with an S-profile, and it was shown in both simulations and experiments that the positive streamer propagation mechanism on an R-profile with 0.5x0.5 mm planar dimensions inhibited positive streamer propagation. See [14] for a more detailed analysis of the propagation mechanism on such profiles.

In Fig. 7, high-speed images show the discharge activity before the voltage collapse (breakdown) for both cylinders. For the non-profiled surface image in Fig. 7b, the discharges seem to stick to the surface. For the profiled surface image in Fig. 7a, on the other hand, the main discharge activity is in the air volume, and not along the surface. There may also be connecting negative streamers from the live electrode in Fig. 7a, which are wider and more diffuse than the positive streamers that propagate from the ground electrode. The images in Fig. 7 are taken at different voltage levels and are therefore not directly comparable. The applied voltage in Fig. 7b is above the $U_{100\%}$ for

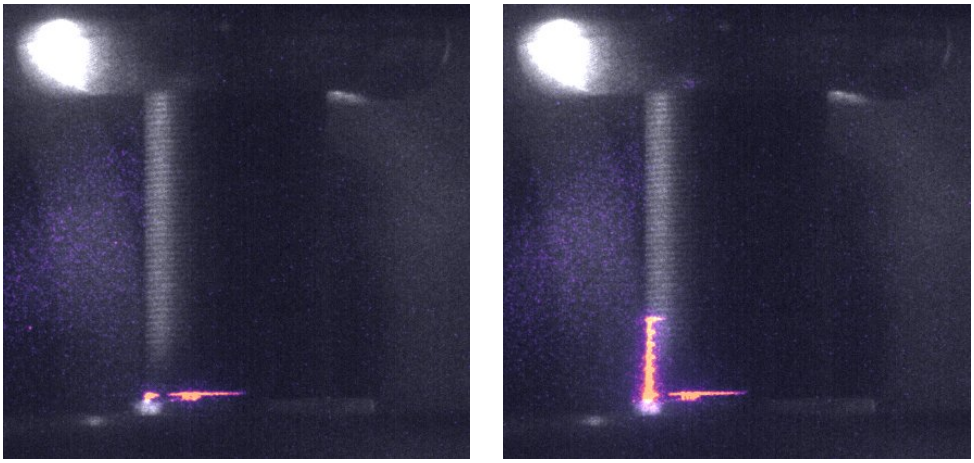

(a) (b)

Figure 5: Surface discharges stopping on the surface profile. a) and b) high-speed images of streamers stopping on profiled surface, no breakdown occurring, 73.5 kV applied, 100 μs exposure, f/2.8 aperture and high image intensifier gain. The triple junction is on the left side of the image.

the non-profiled cylinder, while in Fig. 7a it is below $U_{10\%}$ for the profiled cylinder. Note the many surface discharge channels starting from several discrete locations the ground electrode in Fig. 7b. As the cylinder is stressed with an overvoltage in Fig. 7b, the streamer discharges may also incept from the non-exposed triple-junctions on the ground side. The degree of streamer branching along the non-profiled cylinder surface is relatively low compared to typcal airborne positive streamers in ambient air. Note also the airborne discharges starting from the sharp ground electrode, which can be seen on the lower right-hand side of the test object in the image. The oscilloscope traces in Fig. 6b show that the discharges are occurring on the LI front, and that the camera shutter was closed right before the voltage collapse, but after the discharge inception as seen on the PMT signal.

For the non-profiled cylinder, all observed discharge activity resulted in breakdown. I.e., once streamers initiated from the triple junction, they easily traversed the non-profiled cylinder surface and caused flashover.

3.3 Streamer inception

Fig. 8 shows electric field simulations and streamer inception calculations using eq. 1 near the exposed triple junction. The coloring of the sharp ground electrode shows interpolated inception voltages from electric field

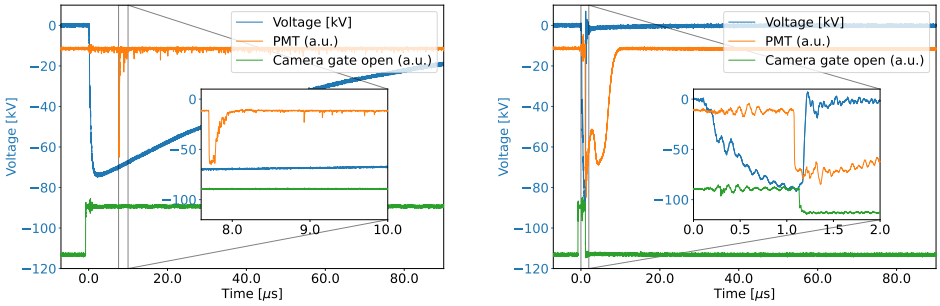

Figure 6: Oscilloscope traces of measured voltage in kV, PMT signal and camera gate opening signals in arbitrary units (a.u.), with inset plots showing the time interval around around the discharge event. a) discharge event where a discharge stops on the profile (image of discharge in Figure 5b) and b) flashover on non-profiled insulator (Figure 7b).

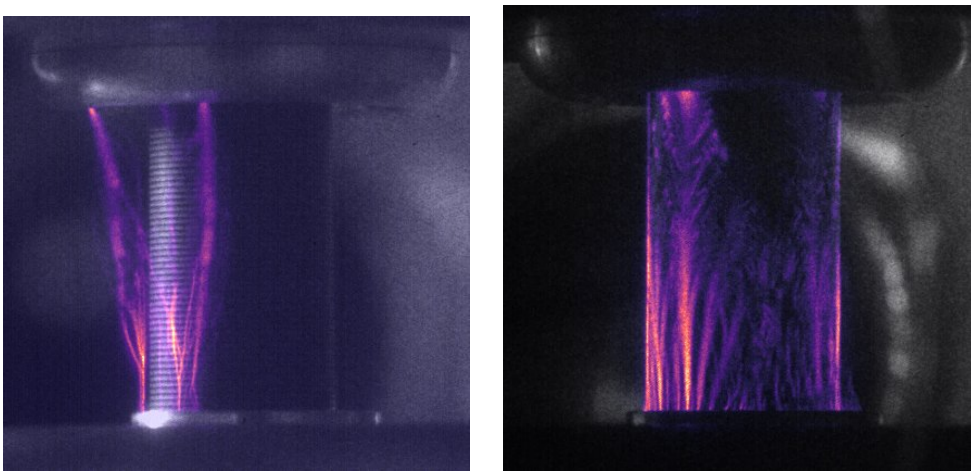

Figure 7: Surface discharges right before breakdown, images taken with f/8 aperture and low image intensifier gain. a) high-speed image right before breakdown on profiled surface, 83 kV prospective voltage peak, 2.8 μs exposure time b) high-speed image right before breakdown at 96 kV prospective voltage peak, non-profiled surface, 1.9 μs exposure time. The triple junction is on the left side of the image.

lines starting from different points on the electrode. 30000 fieldlines were evaluated, 1000 of which are plotted as black streamlines in in Fig. 8a. Two different positions of the profiles relative to the edge are included (Fig. 8c

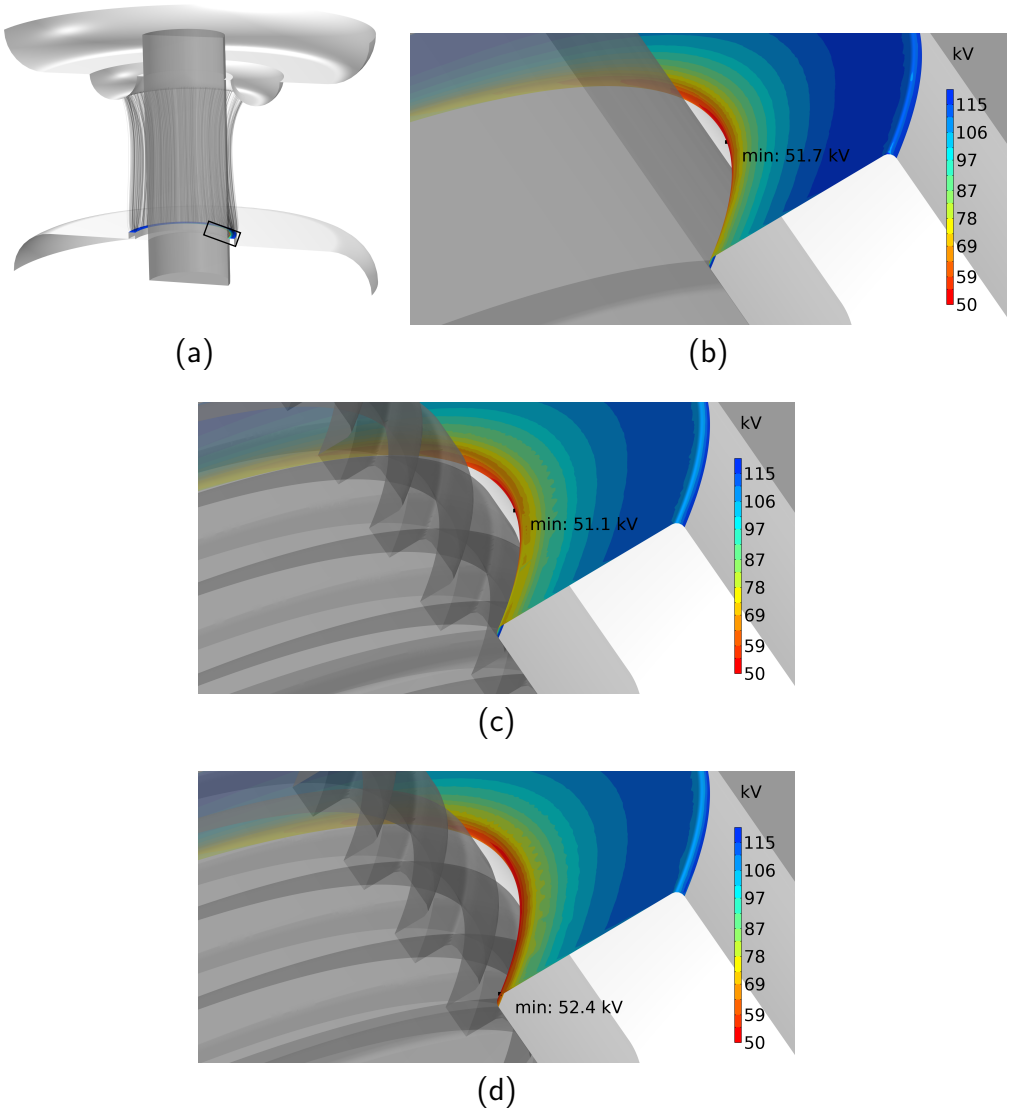

Figure 8: Calculated inception voltages from the asymmetrical grounded electrode edge. a) View of setup with electric field lines from the electrode used for calculation with eq. 1. The black rectangle shows the triple junction region shown in b)-d) close-ups of calculated inception voltages from the grounded electrode in the triple junction region with smooth surface, and two different placements of the surface profile relative to the electrode edge.

and 8d), as this has some effect on the streamer inception field. For all the simulations, the minimum inception voltage U_{inc} was just above 50 kV, but with different locations of the critical field line.

As the inception voltage is the minimum voltage where inception can

occur when a start electron is present at the right place and time, U_{inc} is expected to be significantly lower than $U_{50\%}$ in an inhomogeneous field. For comparison with the experimental data in Fig. 4, the $U_{50\%} - 3\sigma$ (3 standard deviations) on the normal distribution fit to the non-profiled cylinder data is around 55 kV.

For the non-profiled surface, Fig. 8b, the critical point on the electrode is not exactly at the triple junction, but at some distance along the inner edge of the electrode, where the electron avalanches have more room to grow and where the field enhancement from the nearby dielectric is still strong. This is also the case in Fig. 8c where the electrode edge is facing the solid dielectric. In Fig. 8d, on the other hand, the electrode edge is facing an air gap in the profile, so then the critical point is close to where the edge meets the cylinder.

For the profiled surface, positive streamers that start near critical inception points can be arrested on the profile as seen in Fig. 5. In both images in Fig. 5, there are two visible surface streamers near the triple junction. This suggests that the triple junction position relative to the surface profile is more like the simulation in Fig. 8c than the one in Fig. 8d.

The increased withstand voltage of the profiled surface observed in Fig. 4 is a result of the profiles stopping surface streamers that start from the triple junction region. Then, streamer inception from other regions of the electrode is required for breakdown to occur. The other parts of the electrode require higher voltages for streamer inception as shown in Fig. 8c and 8d. As a result, the micro-scale surface profiles inhibit streamer propagation and increase flashover voltage without changing the streamer inception field much in this geometry. In general, such profiles can be applied without introducing major changes to the insulator or electrode geometry or material.

Limitations of the simulations include mechanical tolerances on the test object parts, i.e. that the electrode edge radius is not 0.1 mm everywhere and that there can be small air gaps at triple junctions which are not modelled. With a 0.1 mm sharp metal edge, even 0.1 mm air gaps to the dielectric can strongly reduce the inception voltage at a triple junction, as the avalanches have more room to grow compared to a tightly attached triple junction. But, with the asymmetrical electrode used here, such a gap would not change the inception voltage much as such small air gaps are anyway present. Another limitation of the modelling in Fig. 8 is that the effect of residual surface and space charges from discharges is not modelled.

4 Conclusions

In this work, a new type of micro-scale surface profile which inhibits streamer propagation has been applied to increase the LI flashover voltage of a cylindrical insulator in a 48.5 mm air gap. The surface profile consists of small-scale (0.5x0.4 mm) rectangular grooves in the insulator surface. The groove dimensions were chosen on the basis of previous work involving high-speed imaging and plasma simulations. The insulating cylinder was stressed with an exposed triple junction as the positive electrode. A non-profiled cylinder and a cylinder with a non-streamer-inhibiting surface profile were used as a reference. By stopping streamer discharge propagation, the surface profiles shield the triple junction in the tested electrode configuration, resulting in a significantly increased withstand voltage. High-speed images and electrostatic simulations were presented to explain this effect. The high-speed images showed that the rectangular micro-profiles stopped positive streamers that started close to the triple junction and propagate along the cylinder surface. Images of discharges right before the breakdown revealed details of the flashover mechanism.

The results are relevant for high-voltage applications involving electrically stressed solid insulators in gases, for example in metal-enclosed switchgear insulation design. Such profiles can be especially useful for gaseous insulation systems where a higher flashover voltage is desired, and where only minor changes to the solid insulator materials, geometry, and electrode geometry are feasible.

5 Acknowledgments

This work was funded by the Research Council of Norway and ABB Electrificaton Norway AS through the project "Dielectric solutions for solid insulating components in eco-efficient medium-voltage switchgear" (project number: 321449). The authors thank Andreas Blaszczyk and Nina Sasaki Støa-Aanensen for discussions.

References

[1] A. Pedersen and A. Blaszczyk, "An engineering approach to computational prediction of breakdown in air with surface charging effects," *IEEE Transactions on Dielectrics and Electrical Insulation*, vol. 24, no. 5, pp. 2775–2783, Oct. 2017.

[2] H. Kojima, K. Hotta, T. Kitamura, N. Hayakawa, A. Otake, K. Kobayashi, T. Kato, T. Rokunohe, and H. Okubo, "Classification of impulse breakdown mechanisms under non-uniform electric field in air," *IEEE Trans. Dielect. Electr. Insul.*, vol. 23, no. 1, pp. 194–201, Feb. 2016. [Online]. Available: http://ieeexplore.ieee.org/document/7422560/

[3] M. Seeger, T. Votteler, J. Ekeberg, S. Pancheshnyi, and L. Sanchez, "Streamer and leader breakdown in air at atmospheric pressure in strongly non-uniform fields in gaps less than one metre," *IEEE Trans. Dielect. Electr. Insul.*, vol. 25, no. 6, pp. 2147–2156, Dec. 2018. [Online]. Available: https://ieeexplore.ieee.org/document/8561318/

[4] N. Allen and P. Mikropoulos, "Surface profile effect on streamer propagation and breakdown in air," *IEEE Trans. Dielect. Electr. Insul.*, vol. 8, no. 5, pp. 812–817, Oct. 2001. [Online]. Available: http://ieeexplore.ieee.org/document/959708/

[5] H. K. Meyer, F. Mauseth, R. Marskar, A. Pedersen, and A. Blaszczyk, "Streamer and surface charge dynamics in non-uniform air gaps with a dielectric barrier," *IEEE Transactions on Dielectrics and Electrical Insulation*, vol. 26, no. 4, pp. 1163–1171, Aug. 2019.

[6] C. Ren, B. Huang, C. Zhang, B. Qi, W. Chen, and T. Shao, "Impact of surface charges on energy deposition in surface dielectric barrier discharge: a modeling investigation," *Plasma Sources Sci. Technol.*, vol. 32, no. 2, p. 025004, Feb. 2023, publisher: IOP Publishing. [Online]. Available: https://dx.doi.org/10.1088/1361-6595/acb4b9

[7] X. Meng, L. Wang, H. Mei, B. Cao, and X. Bian, "Streamer Propagation along the Insulator with the Different Curved Profiles of the Shed," *Polymers*, vol. 14, no. 5, p. 897, Jan. 2022, number: 5 Publisher: Multidisciplinary Digital Publishing Institute. [Online]. Available: https://www.mdpi.com/2073-4360/14/5/897

[8] M. Zhu, J. Xue, Y. Wei, G. Li, and G. Zhang, "Review of interface tailoring techniques and applications to improve insulation performance," *High Voltage*, vol. 7, no. 1, pp. 12–31, 2022, _eprint: https://onlinelibrary.wiley.com/doi/pdf/10.1049/hve2.12094. [Online]. Available: https://onlinelibrary.wiley.com/doi/abs/10.1049/hve2.12094

[9] Y. Zhao, Y. Xiang, S. Gu, B. Du, B. Dong, N. Xiang, and H. Xu, "Effect of surface roughness on flashover characteristics of silicone rubber," *Journal of Electrostatics*, vol. 99, pp. 41–48, May 2019.

[Online]. Available: https://www.sciencedirect.com/science/article/pii/S0304388619300026

[10] X. Meng, H. Mei, F. Yin, and L. Wang, "The Development of the Streamer discharge to Flashover along the Dielectric Surfaces," *IEEE Transactions on Dielectrics and Electrical Insulation*, pp. 1–1, 2023, conference Name: IEEE Transactions on Dielectrics and Electrical Insulation.

[11] Y. Huo, W. Liu, C. Ke, C. Chang, and C. Chen, "Sharp improvement of flashover strength from composite micro-textured surfaces," *Journal of Applied Physics*, vol. 122, no. 11, p. 115105, Sep. 2017. [Online]. Available: https://doi.org/10.1063/1.4991934

[12] T. S. Sudarshan and R. A. Dougal, "Mechanisms of Surface Flashover Along Solid Dielectrics in Compressed Gases: a Review," *IEEE Transactions on Electrical Insulation*, vol. EI-21, no. 5, pp. 727–746, Oct. 1986, conference Name: IEEE Transactions on Electrical Insulation.

[13] H. K. H. Meyer, R. Marskar, H. Gjemdal, and F. Mauseth, "Streamer propagation along a profiled dielectric surface," *Plasma Sources Sci. Technol.*, 2020. [Online]. Available: http://iopscience.iop.org/10.1088/1361-6595/abbae2

[14] H. K. H. Meyer, R. Marskar, and F. Mauseth, "Evolution of positive streamers in air over non-planar dielectrics: experiments and simulations," *Plasma Sources Sci. Technol.*, vol. 31, no. 11, p. 114006, Nov. 2022, publisher: IOP Publishing. [Online]. Available: https://dx.doi.org/10.1088/1361-6595/aca0be

[15] H. K. Meyer, R. Marskar, H. Bilsbak, F. Mauseth, and M. Schueller, "Streamer propagation along profiled insulator surfaces under lightning impulse voltages," in *Proceedings of the 27th Nordic Insulation Symposium (in press)*, Jun. 2022.

[16] P. Simka, E.-M. Borrelli, and A. Blaszczyk, "Air Breakdown at Sharp Edges," in *2018 IEEE 2nd International Conference on Dielectrics (ICD)*, Jul. 2018, pp. 1–4.

[17] W. Hauschild and W. Mosch, *Statistical Techniques for High-Voltage Engineering*. IET Digital Library, Jan. 1992. [Online]. Available: https://digital-library.theiet.org/content/books/po/pbpo013e

[18] K. Petcharaks, "Applicability of the streamer breakdown criterion to inhomogenous gas gaps," PhD Thesis, ETH Zurich, 1995.